Anal Bioanal Chem (2017) 409:4257–4266
DOI 10.1007/s00216-017-0376-9

RESEARCH PAPER

Design and development of amperometric biosensor for the detection of lead and mercury ions in water matrix—a permeability approach

Manju Bhargavi Gumpu[1,2] · **Uma Maheswari Krishnan**[3] · **John Bosco Balaguru Rayappan**[1,2]

Received: 3 February 2017 / Revised: 22 March 2017 / Accepted: 21 April 2017 / Published online: 20 May 2017

Abstract Intake of water contaminated with lead (Pb^{2+}) and mercury (Hg^{2+}) ions leads to various toxic effects and health issues. In this context, an amperometric urease inhibition-based biosensor was developed to detect Pb^{2+} and Hg^{2+} ions in water matrix. The modified Pt/CeO_2/urease electrode was fabricated by immobilizing CeO_2 nanoparticles and urease using a semi-permeable adsorption layer of nafion. With urea as a substrate, urease catalytic activity was examined through cyclic voltammetry. Further, maximum amperometric inhibitive response of the modified Pt/CeO_2/urease electrode was observed in the presence of Pb^{2+} and Hg^{2+} ions due to the urease inhibition at specific potentials of −0.03 and 0 V, respectively. The developed sensor exhibited a detection limit of 0.019 ± 0.001 μM with a sensitivity of 89.2 × 10^{-3} μA $μM^{-1}$ for Pb^{2+} ions. A detection limit of 0.018 ± 0.003 with a sensitivity of 94.1 × 10^{-3} μA $μM^{-1}$ was achieved in detecting Hg^{2+} ions. The developed biosensor showed a fast response time (<1 s) with a linear range of 0.5–2.2 and 0.02–0.8 μM for Pb^{2+} and Hg^{2+} ions, respectively. The modified electrode offered a good stability for 20 days with a good repeatability and reproducibility. The developed sensor was used to detect Pb^{2+} and Hg^{2+} ions contaminating Cauvery river water and the observed results were in good co-ordination with atomic absorption spectroscopic data.

Keywords Amperometry · Urease · Enzyme inhibition · Metal ions · Lead and mercury

Introduction

Heavy metal ions such as lead (Pb^{2+}) and mercury (Hg^{2+}) are the common toxicants [1–3], highly persistent in nature and their unique properties such as malleability, ductility, softness, resistance to corrosion and low melting point [4] have enhanced their usage for various industries like automobiles, ceramics, paints and plastics [5]. These metal ions are non-degradable [6] and are considered as potential hazardous substances by the Agency for Toxic Substances and Disease Registry (ATSDR) [7, 8]. Consumption of heavy metal ions contaminated water leads to acute and chronic poisoning with symptoms such as muscle pain, fatigue, abdominal pain, headache, convulsions, vomiting, coma and lethargy [9–11]. In view of these toxic effects, the World Health Organization (WHO), International Agency for Research and Cancer (IARC) and Bureau of Indian Standards (BIS) have limited the permissible limit of Pb^{2+} and Hg^{2+} ions as 50 and 1 μg L^{-1} respectively [12].

Conventional methods such as atomic absorption spectroscopy (AAS) [13, 14], ion chromatography [15], chemiluminescence and inductively coupled plasma mass spectroscopy (ICP-MS) are being used to detect Pb^{2+} and Hg^{2+} ions contamination in water. All these techniques are limited due to expensive instrumentation, time-consuming process and requirement of a highly skilled man power [16–18]. To overcome these limitations,

Electronic supplementary material The online version of this article (doi:10.1007/s00216-017-0376-9) contains supplementary material, which is available to authorized users.

✉ John Bosco Balaguru Rayappan
rjbosco@ece.sastra.edu

[1] Nano Sensors Lab, Centre for Nanotechnology & Advanced Biomaterials (CeNTAB), SASTRA University, Thanjavur, Tamil Nadu 613 401, India

[2] School of Electrical & Electronics Engineering, SASTRA University, Thanjavur, Tamil Nadu 613 401, India

[3] School of Chemical and Biotechnology, SASTRA University, Thanjavur, Tamil Nadu 613 401, India

electrochemical biosensor is used due to its rapidity, portability, sensitivity, and ease of analysis [19–22].

To detect Pb^{2+} ions in water matrix, Illangovan [23] developed an urease inhibition-based biosensor with a linear range of 0.1–1 mM, but with a limited stability [23]. Shen et al. [24] have developed an electrochemical biosensor to detect Pb^{2+} ions using the modified gold electrode by attaching the oligonucleotides to gold nanoparticles. In spite of its lower detection limit (LOD) of 1 nM, background current lead to direct oxidation of nucleotides, which resulted in inaccurate estimation. Apart from urease, enzymes like invertase [25], horse radish peroxidase (HRP), tyrosinase, acetyl cholinesterase (AChE) and glucose oxidase (GOD) [26–28] were also utilized to develop biosensors to detect Pb^{2+} and Hg^{2+} ions. Various interfaces such as poly-*o*-phenylenediamine (PPD) [29], ZnO nanoparticles [26], poly neutral red (PNR)-modified carbon film, etc. were employed in various electrochemical biosensors. But, majority of these approaches have limitations in terms of response time, stability and precision. Hence, it is important to design and develop biosensor for the selective detection of Pb^{2+} and Hg^{2+} ions in water matrix with lower detection limit and high stability.

In this work, an electrochemical urease inhibition-based biosensor has been developed to detect Pb^{2+} and Hg^{2+} ions in water using ceria (CeO_2) nano-interface. The higher differences in isoelectric points (IEP) of urease (IEP = 4.9) and CeO_2 (IEP = 9.2) provided strong electrostatic interaction between enzyme and nano-interface [30]. The usage of CeO_2 nano-interface helped in enhancing direct electron transfer kinetics owing to its unique properties such as high surface to volume ratio, surface reactivity, adsorption rate and catalytic activity. Tuning potential window for selective detection of Pb^{2+} and Hg^{2+} ions at lower potentials is the major highlight of this work. Reliability of the developed Pt/CeO_2/urease electrode was proved by optimizing various experimental conditions for the selective amperometric detection of Pb^{2+} and Hg^{2+} ions in contaminated water samples.

Experimental

Chemicals and reagents

Urease (E.C.) from *Canavalia ensiformis* (E.C. 3.5.1.5, activity: 15 U mg^{-1}), cerium acetate dehydrate, sodium chloride, hydrosulfuric acid, sodium citrate, citric acid, lead nitrate, cadmium acetate, cobalt acetate, zinc chloride, mercuric sulphate, arsenic (III) iodide, urea, ethylenediaminetetraacetic acid (EDTA), nickel nitrate, iron chloride, calcium carbide, potassium acetate and nafion were procured from Sigma-Aldrich, India. All the studies were carried out at room temperature using deionized water of conductivity <1 μ mho, pH 5.6. Citrate buffer of 0.1 M with pH ranging from 4 to 10 were prepared by dissolving appropriate amount of sodium citrate and citric acid in 100 mL of deionized water.

Details on apparatus, synthesis and characterization of CeO_2 nanoparticles are included in the Electronic Supplementary Material (ESM) in sections 1 and 2.

Fabrication of Pt-modified working electrode

Pt electrode was polished using alumina powder and subsequently cleaned electrochemically. During this cleaning process, Pt electrode was scanned in the potential range of 0 to 0.8 V *vs Ag/AgCl* in 0.1 M H_2SO_4 at 0.1 Vs^{-1}. For the fabrication of modified Pt electrode, CeO_2 nanoparticles (0.1 mg mL^{-1}) were dispersed in deionized water and sonicated for 15 min. Then, 3 μL of CeO_2 dispersed solution was drop casted on to the Pt electrode. Subsequently, 100 μL of urease (0.1 U mL^{-1}) was dispersed along with 5 μL of nafion (0.5 (*v*/*v*)) solution and this mixture was coated on to the CeO_2embedded Pt electrode surface and air dried for 30 min (Fig. 1).

Procedure for urea determination

The steady state of urea interaction with urease was measured in terms of current response recorded in the presence of 0.1 M citrate buffer (pH 6) in the range of −0.2 to 0.8 V vs Ag/AgCl. The concentration studies were performed by increasing the urea levels till saturation.

Electrochemical estimation of Pb^{2+} and Hg^{2+} ions

At the saturating concentration of urea, inhibitive response of Pb^{2+} and Hg^{2+} ions was evaluated based on the percentage inhibition (Eq. (1)). Besides, the analytical parameters of the developed sensor such as LOD, sensitivity and linear range were estimated. Reusability of the developed sensing element was studied in terms of reactivation (Eq. (2)) using 0.1 M EDTA. Finally, the fabricated electrode was used to detect Pb^{2+} and Hg^{2+} ions in Cauvery river water (filtered using a filter paper of 0.45 mm pore size) and the observed results were validated using AAS.

$$\text{Inhibition } (I\%) = \frac{(I_0 - I_i)}{I_0} \times 100 \quad (1)$$

where I_0 and I_i represent the current response of urea on Pt/CeO_2/urease electrode without and with Pb^{2+} and Hg^{2+} ions.

$$\text{Reactivation } (R\%) = \frac{I_r - I_{p,\text{exp}}}{I_{p,\text{control}} - I_{p,\text{exp}}} \times 100 \quad (2)$$

where I_r is the current response of urea on Pt/CeO_2/urease electrode with EDTA reactivation, $I_{p,exp.}$ is the current response of urea on Pt/CeO_2/urease electrode with metal ion

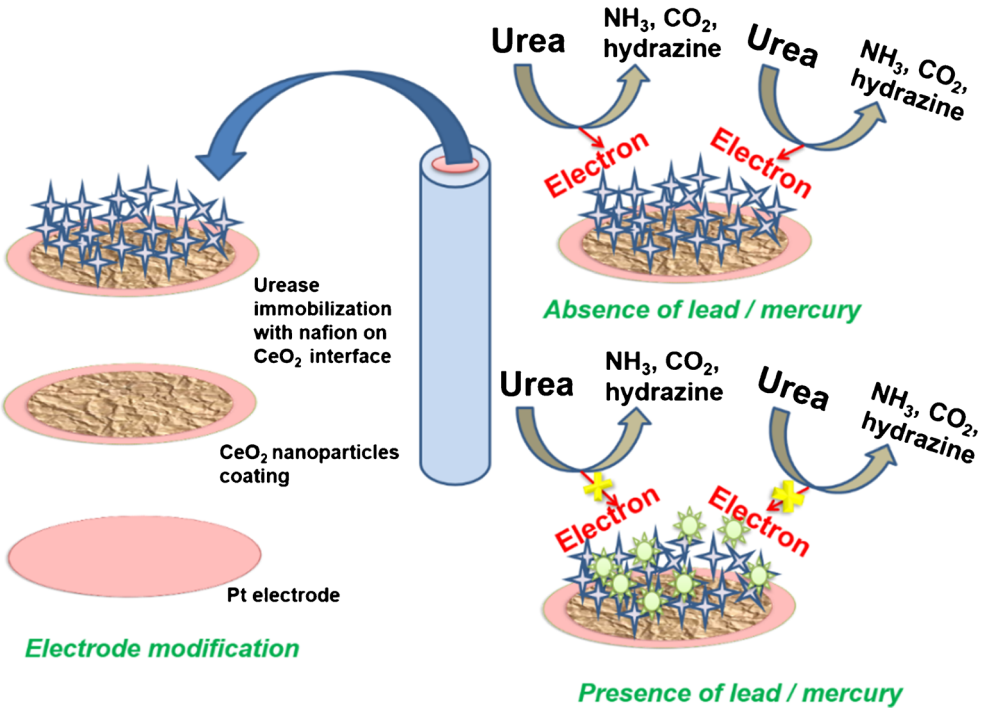

Fig. 1 Schematic representation of Pt electrode modification and inhibition of urease in the presence of Pb^{2+} or Hg^{2+} ions

inhibition and $I_{p,control}$ is the current response of urea on Pt/CeO_2/urease electrode.

Results and discussion

Electrochemical behaviour of the modified electrodes

The initial cyclic voltammetric experiments were conducted using 0.1 M citrate buffer solution with pH 7 as electrolyte. The responses of bare Pt (black), Pt/CeO_2 (red), Pt/urease (green) and Pt/CeO_2/urease (blue) electrodes in the presence of 1.0 μM of urea at a scan rate of 0.1 Vs^{-1} are shown in Fig. 2a. Bare Pt electrode showed no redox peak and the modified electrodes exhibited an oxidation peak at 0 V vs Ag/AgCl, which corresponds to the decomposition of urea to ammonia, carbon dioxide and hydrazine. The reaction mechanism is as follows:

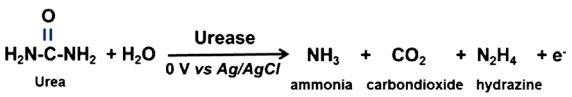

The oxidation current responses of various modified working electrodes were calculated and represented in the ESM in Table S1. Pt/urease, Pt/CeO_2 and Pt/CeO_2/urease electrodes *vs Ag/AgCl* exhibited anodic peak potential (E_{pa}) of −0.03, 0.01 and 0.05 V, respectively. Pt/urease, Pt/CeO_2 and Pt/CeO_2/urease electrodes showed a maximum anodic peak current (I_{pa}) of 3.51, 3.63 and 3.96 μA, respectively. This has confirmed the catalytic activity of modified electrode. Pt/CeO_2 also exhibited an oxidation peak owing to the dual reversible oxidation state of cerium Ce(III)/Ce(IV) redox couple and hence, urea get oxidized to ammonia, carbon dioxide and hydrazine. (Mechanism is given in the ESM in section 3). The lower electron transfer rate of Pt/CeO_2 was confirmed by its large full width half maximum (FWHM = 62.5 mV/nαA, where n is the number of electrons transferred (n = 1), α is the electron transfer coefficient (α = 0.5) and A is the area of Pt working electrode (0.0314 cm^2)). The calculated electron transfer rate constant ($K_s = I_{pa}/Q$, where I_{pa} is the anodic peak current and Q is the amount of charge consumed) is given in Table S1 (see ESM). Considering increased current response, enhanced electron transfer of Pt/CeO_2/urease over Pt/urease and Pt/CeO_2, Pt/CeO_2/urease electrode was used for further electrochemical studies. The experimental conditions like electrolyte, pH, scan rate, urease loading efficiency and urea concentration were optimized and the related information is given in the ESM in section 4.

Determination of Pb^{2+} and Hg^{2+} ions by an inhibition process

The response of biosensor was recorded in 0.1 M citrate buffer (pH 6) at a scan rate of 0.08 Vs^{-1}. With an increase in urea concentration ranging from 0.1 to 1.8 μM, an increase in current response was observed at 0 V *vs Ag/AgCl* and reached saturation at 1.5 μM (Fig. 2b). To the saturated concentration of urea, addition of Pb^{2+} and Hg^{2+} ions of various concentrations (0.05, 0.08, 0.1, 0.5, 0.8, 1.0, 1.5, 2.0, 2.5, 3.0 μM) lead

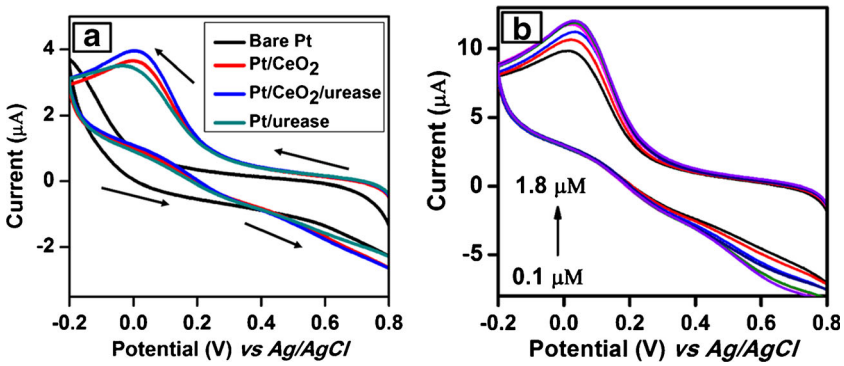

Fig. 2 **a** Cyclic voltammograms of bare and various modified Pt electrode in 0.1 M citrate buffer (pH 7), scan rate of 0.1 Vs^{-1} containing 1.0 μM of urea and **b** CVs of Pt/CeO_2/urease in the presence of 0.1 M citrate buffer (pH 6), scan rate of 0.08 Vs^{-1} with varying concentrations of urea

to a decrease in current response (Fig. 3a). This trend might be due to the inhibition of active sites of urease by metal ions (see ESM, section 5). This inhibition is facilitated by the natural affinity between Ni metallic center of urease and soft base target ions (Pb^{2+} and Hg^{2+}). As both the metal ions are selective towards urease (see ESM, Fig. S3A-D), the ability of the active sites to discriminate the particular metal ion from a mixture of metal ions has become crucial. Hence, to selectively detect the target ions, amperometric studies were carried out for the varying concentrations of Pb^{2+} (0.05 to 3 μM) and Hg^{2+} (0.05 to 3 μM) ions at various oxidation potentials (0, −0.03, 0.03, −0.05 and 0.05 V *vs Ag/AgCl*) in the presence of 1.5 μM of urea, 0.1 M of citrate buffer (pH 6). Similar to voltammetric studies, amperometric studies also exhibited a decreased current response with an increase in concentration of Pb^{2+} and Hg^{2+} ions. It was evident from Fig. 3b that amperogram at −0.03 V *vs Ag/AgCl* exhibited a 95.2% inhibition for Pb^{2+} and 97.1% for Hg^{2+} at 0 V *vs Ag/AgCl* (Fig. 3c). This variation in potentials was greatly influenced by the permeability of metal ions. Hence, the permeability of Ni^{2+}, Fe^{3+}, Co^{2+}, Ca^{2+}, Zn^{2+}, K^{+}, Cd^{2+}, Cr^{3+}, Cu^{2+}, Pb^{2+}, Hg^{2+} and As^{3+} ions (0.5 μM) was calculated using Eqs. (4) and (5) and presented in Fig. 3d.

$$P\,[S]\% \;=\; \frac{\text{Slope } M \text{ at } Pt/CeO_2/\text{urease}}{\text{Slope } M \text{ at bare } Pt} \times 100 \qquad (4)$$

where M = Pb^{2+} *or* Hg^{2+} ions

$$P\,[I]\% = \frac{I_{\text{interfernt}}\ (0.5\,\mu\text{M})\ \text{at}\ Pt/CeO_2/\text{urease}}{I_{\text{interferent}}\ (0.5\,\mu\text{M})\ \text{at bare}\ Pt} \times 100 \qquad (5)$$

Permeabilities of Pb^{2+} and Hg^{2+} ions were observed to be 4 and 1.2 times greater than that of Fe^{3+}, Co^{2+}, Ca^{2+}, Zn^{2+}, K^{+}, Cd^{2+}, Cr^{3+} and As^{3+} ions at −0.03 and 0 V vs Ag/AgCl, respectively. Also, amperometric selectivity coefficient (Eq. (6)) and response ratio (Eq. (7)) of mixed metal ion solutions (Table 1) were evaluated at −0.03 and 0 V *vs Ag/AgCl*.

$$\text{Amperometric selectivity coefficient}\left(K_{i,j}^{amp}\right) = \frac{\Delta I_j}{\Delta I_t - \Delta I_j} \times \frac{\Delta C_i}{\Delta C_j} \qquad (6)$$

$$\text{Response ratio}\ \left(R_{i,j}\right) = \frac{\Delta I_j}{\Delta I_i} \qquad (7)$$

where $^{\triangle}I_i$ is the amperometric current response of analyte solution, $^{\triangle}I_j$ is the amperometric current response of interfering cation solution, $^{\triangle}I_t$ is the amperometric current response of the mixed solution, C_i is the concentration of analyte of interest and C_j is the concentration of interfering cation.

The lower values of amperometric selectivity coefficient and response ratio of Pt/CeO_2/urease electrode at −0.03 V *vs Ag/AgCl* in the presence of interferents confirmed the selectivity towards Pb^{2+} ions. Similarly at 0 V *vs Ag/AgCl*, the amperometric selectivity coefficient and response ratio of Pt/CeO_2/urease electrode were observed to be very low including Pb^{2+} ions. The estimated analytical parameters of Pb^{2+} and Hg^{2+} ion biosensor are presented in Table 2.

Interferent study

Selective nature of Pb^{2+} and Hg^{2+} towards Pt/CeO_2/urease electrode was tested in the presence of other metals namely Fe^{3+}, Co^{2+}, Ca^{2+}, Zn^{2+}, K^{+}, Cd^{2+}, Cr^{3+}, As^{3+} and Ni^{2+} (0.5 μM) (Fig. 3e). All these metal ions showed an inhibition

Fig. 3 **a** Cyclic voltammograms of Pt/CeO_2/urease electrode in the ▶ presence of 1.5 μM of urea, citrate buffer (pH 7) by varying Pb^{2+} and Hg^{2+} ion concentrations; amperometric determination of **b** Pb^{2+} and **c** Hg^{2+} ions at various oxidation potentials, **d** permeability, **e** selectivity of Hg^{2+} and Pb^{2+} ions and **f** mechanism of urea and urease interaction in the absence and presence of Pb^{2+} and Hg^{2+} ions

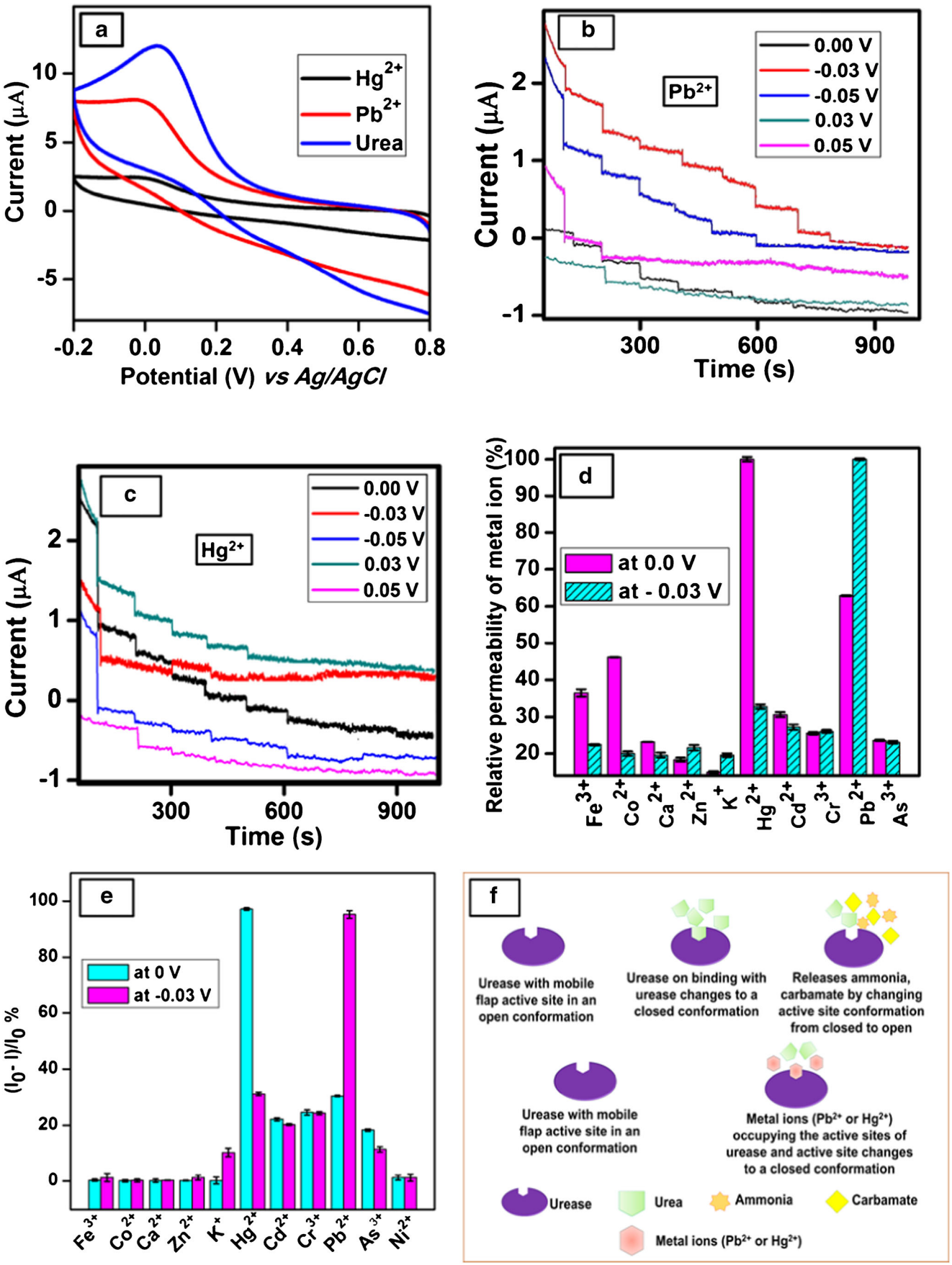
a
Current (μA)
Potential (V) vs Ag/AgCl
Hg2+
Pb2+
Urea
b
Pb2+
0.00 V
-0.03 V
-0.05 V
0.03 V
0.05 V
Current (μA)
Time (s)
c
Hg2+
0.00 V
-0.03 V
-0.05 V
0.03 V
0.05 V
Current (μA)
Time (s)
d
at 0.0 V
at - 0.03 V
Relative permeability of metal ion (%)
Fe3+ Co2+ Ca2+ Zn2+ K+ Hg2+ Cd2+ Cr3+ Pb2+ As3+
e
at 0 V
at -0.03 V
(I0- I)/I0 %
Fe3+ Co2+ Ca2+ Zn2+ K+ Hg2+ Cd2+ Cr3+ Pb2+ As3+ Ni2+
f
Urease with mobile flap active site in an open conformation
Urease on binding with urease changes to a closed conformation
Releases ammonia, carbamate by changing active site conformation from closed to open
Urease with mobile flap active site in an open conformation
Metal ions (Pb2+ or Hg2+) occupying the active sites of urease and active site changes to a closed conformation
Urease
Urea
Ammonia
Carbamate
Metal ions (Pb2+ or Hg2+)

Table 1 Interference studies of mixed and separate solution response

Interferent	Pb^{2+}		Hg^{2+}	
	Amperometric selectivity coefficient, $K_{i,j}^{amp}$ $(\times 10^{-3})$	Response ratio, $R_{i,j}(\times 10^{-3})R_{i,j}$	Amperometric selectivity coefficient, $K_{i,j}^{amp}$ $(\times 10^{-3})$	Response ratio, $R_{i,j}(\times 10^{-3})$
As^{3+}	0.436	0.304	0.562	0.042
Fe^{3+}	0.496	0.303	0.212	0.113
Co^{2+}	0.392	0.302	0.312	0.726
Ca^{2+}	0.449	0.309	0.874	0.523
Zn^{2+}	0.452	0.921	0.863	0.654
K^{+}	0.520	0.075	0.525	0.232
Hg^{2+}	0.382	0.022	NA	NA
Cd^{2+}	0.525	0.329	0.132	0.210
Cr^{3+}	0.909	0.317	0.382	0.443
Pb^{2+}	NA	NA	0.112	0.112

of less than 30%, which confirmed the selectivity of the developed sensor towards Pb^{2+} (2.2 μM) and Hg^{2+} (0.8 μM) ions. The ultra-low potential of 0 and −0.03 V *vs Ag/AgCl* offered by Pt/CeO_2/urease electrode helped in avoiding cross reactivity. Besides, amperometric selective coefficients obtained for both the Pb^{2+} and Hg^{2+} ions are in the magnitudes of 10^{-3} demonstrated anti-interferent nature of the Pt/CeO_2/urease electrode.

Mechanism of inhibition and kinetics

Urease is a metallo enzyme rich in cysteine residues with α-subunit containing a binuclear nickel center [31]. While urease mobile flap is in open conformation, urea binds at the active site and changes to a closed conformation. In this case, when urea comes closer to urease, carbon atom of urea comes into close proximity to nickel-binding ligand forming nucleophiles by polarizing C-O and C-NH_2 bonds. In closed conformation, histidine at hydrogen bonding distance forms nascent ammonia and breaks C-N bond which resulted in open conformation [32] (Fig. 3f).

The binding of Pb^{2+} and Hg^{2+} ions at the active sites of urease is based on the hard and soft acids and bases concept (HSAB). These ions belong to class B prefers specifically binding to soft donors such as sulphur, nitrogen and oxygen in a preferential order S > N > O. Once Pb^{2+} or Hg^{2+} binds at the active site, the open flap changes its conformation to closed conformation by blocking urea [1] and hence a decreased current response was observed with an increase in Pb^{2+} and Hg^{2+} concentration.

Since the concentration of urea, Pb^{2+} and Hg^{2+} has a great influence on sensor performance, inhibition kinetics of urease in the presence of Pb^{2+} as well as Hg^{2+} were evaluated. The decreased activity of urease was a result of competitive, mixed inhibition and the same was confirmed from the Lineweaver-Burk plot for Pb^{2+} (Fig. 4a) and Hg^{2+} (Fig. 4b) respectively. Varying concentrations of Pb^{2+} showed a linear trend over the inverse of anodic peak current and the extrapolated linear plot intersected on *Y*-axis, which revealed the value of I_{max}. The K_M values for the concentrations of 0, 0.05, 0.08 and 1.0 μM were found to be 2.419, 2.6, 3.125 and 3.3 μM respectively. This trend proved the competitive inhibition between Pb^{2+} and urea. In the case of Hg^{2+}, extrapolated linear plot intersected at the negative co-ordinates of *X*- and *Y*-axes with decreased I_{max} and increased K_M values revealed the mixed inhibition by Hg^{2+} ions.

The Dixon plot ($1/I_{pa}$ vs lead concentration) at various urea concentrations (0.1, 0.5, 1 μM) showed a linear regression with R^2 = 0.99 and inhibition constant (K_i) of 0.58 and 0.72 μM, respectively, for Pb^{2+} (Fig. 4c) and Hg^{2+} ions (Fig. 4d) (Table 2). This lower inhibition constant revealed the stronger binding force between the target ions and urease-urea complex. The estimated '*n*' value (>1) from Hill plot confirmed the positive co-operativity for both Pb^{2+} and Hg^{2+} ions with R^2 = 0.98.

Table 2 Response characteristics of Pt/CeO_2/urease biosensor

Parameter	Estimated value for Pb^{2+} at −0.03 V	Estimated value for Hg^{2+} at 0 V
Sensitivity	89.2×10^{-3} μA μM^{-1}	94.1×10^{-3} μA μM^{-1}
Linear range	0.5–2.2 μM	0.02–0.8 μM
Degree of inhibition	95.2%	97.1%
I_{max}^{app}	2.5 μA	6.24 μA
K_M^{app}	0.3 μM	0.42 μM
LOD	0.019 ± 0.001 μM	0.018 ± 0.003 μM
IC_{50}	0.88 μM	0.96 μM
K_i	0.58 μM	0.78 μM
Reactivation using EDTA	97.25%	95.02%
Response time	<1 s	<1 s

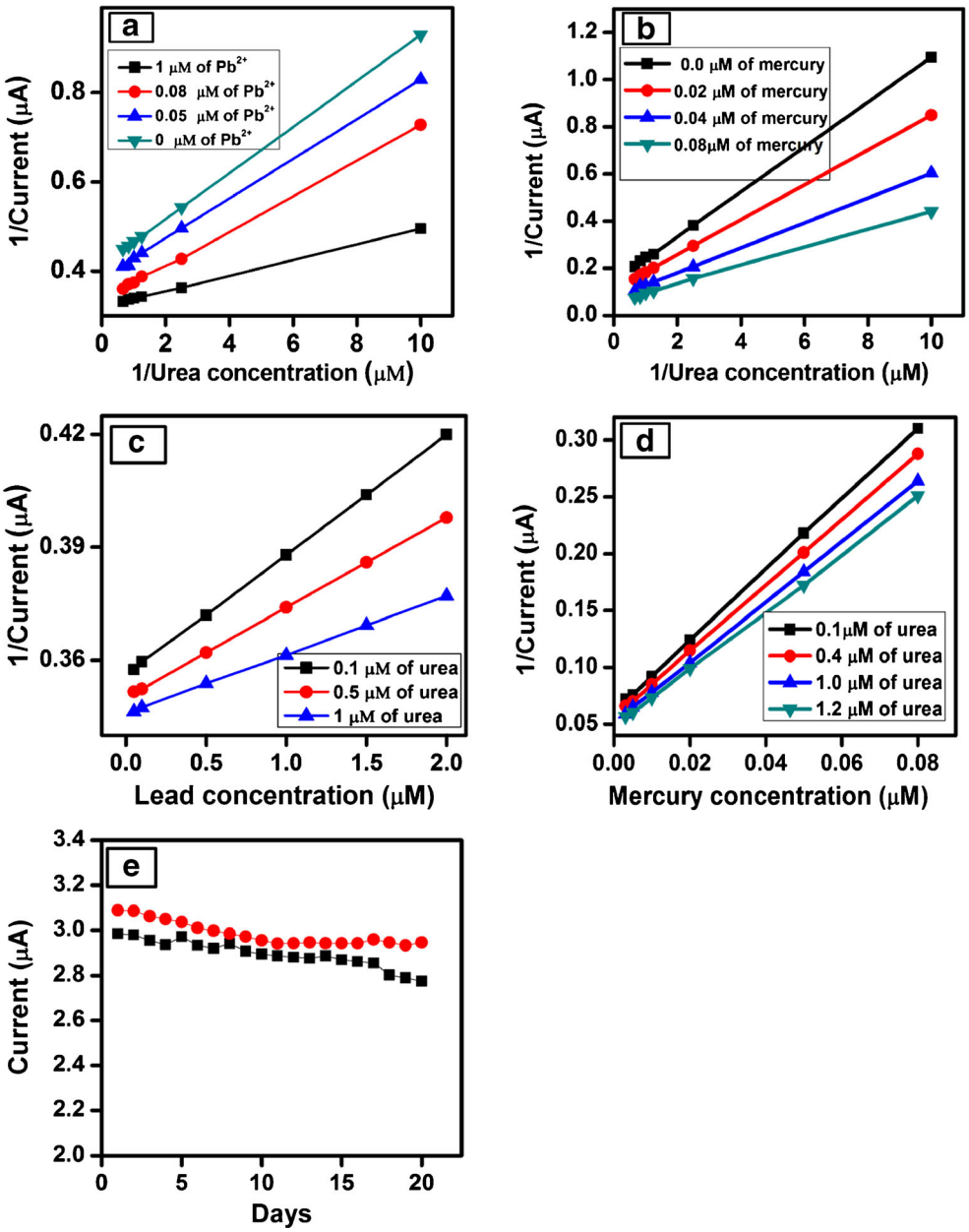

Fig. 4 Lineweaver-Burk plot of **a** Pb^{2+} indicating the competitive inhibition, **b** Hg^{2+} indicating mixed inhibition, **c** Dixon plot of Pb^{2+} inhibition, **d** Dixon plot of Hg^{2+} inhibition and **e** operational stability of Pt/CeO_2/urease in the presence of Pb^{2+} and Hg^{2+} ions

Table 3 Recovery studies of Pb^{2+} Cauvery river water

Sample (100 μL of Cauvery water)	Pb^{2+} added (μM)	Mean Pb^{2+} detected (μM)	Recovery (%)	RSD (%) (n = 5)
1	0.05	0.058	116.00	3.24
2	0.10	0.140	140.00	3.62
3	0.90	0.810	90.00	2.15
4	1.10	1.120	101.81	1.12
5	1.30	1.310	100.77	1.06
6	1.50	1.530	102.10	3.10
7	1.70	1.730	101.76	0.20
8	1.90	1.890	99.47	1.14

Table 4 Recovery studies of Hg^{2+} in Cauvery river water

Sample (100 μL of Cauvery water)	Hg^{2+} added (μM)	Mean Hg^{2+} detected (μM)	Recovery (%)	RSD (%) (n = 5)
1	0.008	0.008	100.00	1.26
2	0.010	0.010	90.00	0.94
3	0.030	0.030	100.00	1.44
4	0.060	0.050	083.33	2.01
5	0.090	0.090	0100.00	0.98
6	0.200	0.190	095.00	2.11
7	0.400	0.410	102.50	2.94
8	0.800	0.790	098.75	1.77

Table 5 Determination of Pb^{2+} and Hg^{2+} in Cauvery river water using the developed sensor and AAS

Metal ion	Proposed method (μM)	AAS (μM)	Relative deviation (%)
Pb^{2+}	22.93 ± 0.21	23.17 ± 0.46	2.35
Hg^{2+}	4.27 ± 0.43	4.48 ± 0.55	3.1

Evaluation of Pt/CeO_2/urease-modified electrode

(a) Reactivation studies: To carry out the reactivation studies, Pt/CeO_2/urease electrode was immersed in 0.1 M EDTA reactivator for 10 min to remove metal ions from the active sites of urease. The EDTA-treated Pt/CeO_2/urease electrode showed a reactivation of 97.25 and 95.02% towards Pb^{2+} and Hg^{2+} respectively.

(b) Repeatability and reproducibility (precision): To evaluate repeatability and reproducibility, five modified Pt/CeO_2/urease electrodes were fabricated to detect Pb^{2+} and Hg^{2+} ions in 0.1 M citrate buffer (pH 6) containing 1.5 μM of urea. Intra-assay (n = 5) of Pt/CeO_2/urease electrode showed an RSD of 0.02 and 0.123% for Pb^{2+} and Hg^{2+} ions, respectively. Inter-assay (n = 5) showed an RSD of 0.057 and 0.283% Pb^{2+} and Hg^{2+} ions respectively. Since RSD was <5%, it can be concluded that the fabricated Pt/CeO_2/urease electrode can be reproduced and deployed for water sample analysis.

(c) Accuracy: accuracy of Pt/CeO_2/urease electrode was tested for various concentrations of Pb^{2+} ions (0.5, 0.8, 1.2, 1.8 and 2.2 μM). The predicted Pb^{2+} concentration ± relative error (n = 5) was calculated as 0.5 ± 0.038, 0.8 ± 0.023, 1.2 ± 0.015, 1.8 ± 0.010 and 2.2 ± 0.008 μM respectively. Similarly for Hg^{2+} ions (0.2, 0.35, 0.5, 0.65 and 0.8 μM), the predictive values were estimated as 0.2 ± 0.09, 0.35 ± 0.05, 0.5 ± 0.036, 0.65 ± 0.027 and 0.8 ± 0.022 μM respectively. The detailed accuracy estimation is presented in the ESM in section 6.

(d) Stability of Pt/CeO_2/urease electrode: the operational stability (Eq. ((8)) of the developed Pt/CeO_2/urease electrode in the presence of 1.5 μM of urea, 1 μM of Pb^{2+} and Hg^{2+} ions was examined for a period of 20 days at room temperature (Fig. 4e). It exhibited an operational stability of 92.94 and 86.7% for Pb^{2+} and Hg^{2+} ions respectively.

$$\%\text{Stability} = 100\left[\frac{I_n - I_0}{I_0}\right] \times 100 \quad (8)$$

where I_0 is the current measured on the first day and I_n on 'nth' day.

Real sample analysis and validation

In India, Cauvery river is considered to be one of the fresh water bodies covering an area of around 72,000 km^2 and has many tributaries. But, in recent years, due to release of untreated effluent from industries and waste disposal, the metal ion concentration has increased [33, 34].

Towards the detection of Pb^{2+} and Hg^{2+} ions in Cauvery river water (TDS = 318 ppm, pH 6.2 and conductivity of 5.5×10^{-6} S m^{-1}) (Tables 3 and 4), standard addition method

Table 6 Comparison of analytical characteristics of the developed Pt/CeO_2/urease sensor with existing biosensors in detecting Pb^{2+} and Hg^{2+} ions

Metal ion	Electrode	LOD ± RSD (μM)	Linear range (μM)	Sensitivity (μA μM^{-1})	Stability	Response time	Ref.
Pb^{2+}	Pristine single-walled carbon nanotube	0.003 ± 4.3	0.0011–0.0015	NM	7 days	NM	[35]
Pb^{2+}	Molecularly imprinted polymers	0.2 ± 3.9	0.3–50	NM	80%	NM	[20]
Pb^{2+}	Immobilized DNA with CeO_2–MWCNT composite	0.005 ± 3.6	0.01–10	NM	95.5%	NM	[36]
Pb^{2+}	Screen-printed bismuth oxide	0.011 ± 0.122	0.096–0.482	NM	NM	NM	[37]
Pb^{2+}	Graphene/ionic liquid composite modified screen-printed electrode	4.826×10^{-4} ± 1.99	0.004–0.386	NM	NM	NM	[38]
Pb^{2+}	CNTs/nafion/aspartic acid modified screen printed electrodes	NM	1–50	5.22	NM	NM	[39]
Pb^{2+}	Polysulfoaminoantroquinone/poly vinyl chloride/dioctyl phthalate	0.16 ± 4.9	0.501–251	29.3 mV $decade^{-1}$	NM	NM	[40]
Hg^{2+}	Platinum ultra microelectrode/invertase	5×10^{-4} ± NM	5×10^{-4}–0.001	NM	57 days	<15	[25]
Pb^{2+}	Platinum ultra microelectrode/invertase	0.03 ± NM	0.05–0.25	NM	57 days	<15	[25]
Hg^{2+}	Urease/Au nanoparticles/SPCE	0.056 ± 0.5	0.006–0.06	NM	NM	NM	[41]
Pb^{2+}	Pt/CeO_2/urease	0.019 ± 0.001	0.5–2.2	89.2×10^{-3}	92.94%	<1	Present work
Hg^{2+}	Pt/CeO_2/urease	0.018 ± 0.003	0.02–0.8	94.1×10^{-3}	86.7%	<1	Present work

was adopted. The acceptable ranges of 91.63–107.09 and 90.00–103.00% were obtained for Pb^{2+} and Hg^{2+} ions respectively (Tables 3 and 4). The validation study was carried out using AAS and the results are given in Table 5.

As the amount of Pb^{2+} and Hg^{2+} ions were present in 100 μL of 100-fold diluted metal ion samples, the concentration of Pb^{2+} and Hg^{2+} ions were estimated using the following equations

$$\text{Metal ion concentration}\left(\mu g/\mu L\right) = \frac{\text{Current}\,(\mu A) \times \text{dilution factor}}{\text{slope}\left(\frac{\mu A}{\mu g}\right) \times \text{volume of diluted metal ion used for the assay}(\mu L)} \quad (9)$$

$$\text{Recovery}\,(\%) = \frac{\text{Mean metal ion detected}}{\text{Metal ion added for the assay}} \times 100 \quad (10)$$

where dilution factor is 100 and volume of diluted metal ion used for the assay is 100 μL.

Also, the observed results were in good agreement with AAS data. The performance comparison of the developed sensor with the available sensors (Table 6) highlights the superior performance in terms of detection limit, linear range and response time of Pt/CeO_2/urease electrode.

Conclusion

This work highlights the fabrication of Pt/CeO_2/urease electrode for the selective detection of Pb^{2+} and Hg^{2+} ions using amperometry. First time, the permeability of Pb^{2+} and Hg^{2+} ions with respect to the applied potential was measured, which could enable a specific potential based discrimination of Pb^{2+} and Hg^{2+} ions in a mixed solution. The ability of the developed electrode to work at lower potentials enabled it to be anti-interferent. The detection limit of the developed sensor towards Pb^{2+} and Hg^{2+} ions is less than WHO limit. In addition, lower response time has proved Pt/CeO_2/urease to be a reliable sensing platform to detect Pb^{2+} and Hg^{2+} ions. The results obtained in quantification of Pb^{2+} and Hg^{2+} ions using the developed Pt/CeO_2/urease electrode are in good agreement with the AAS data. Hence, the developed electrode can be deployed to detect Pb^{2+} and Hg^{2+} ions in water bodies.

Acknowledgements The authors are grateful to the Department of Science & Technology, New Delhi for their financial support (DST/TM/WTI/2K14/197(a)(G)), (SR/FST/ETI-284/2011 (C)), (SR/FST/LSI-453/2010) and (SR/NM/PG-16/2007). We also acknowledge SASTRA University, Thanjavur for extending infrastructure support to carry out the study.

Compliance with ethical standards

Conflict of interest The authors declare that they have no conflict of interest.

References

1. Du N, Chen M, Liu Z, Sheng L, Xu H, Chen S. Kinetics and mechanism of jack bean urease inhibition by Hg^{2+}. Chem Cent J. 2012;6:154. doi:10.1186/1752-153X-6-154.
2. Mohammadi H, Amine A, Cosnier S, Mousty C. Mercury–enzyme inhibition assays with an amperometric sucrose biosensor based on a trienzymatic-clay matrix. Anal Chim Acta. 2005;543:143–9. doi:10.1016/j.aca.2005.04.014.
3. Aragay G, Merkoci A. Nanomaterials application in electrochemical detection of heavy metals. Electrochim Acta. 2012;84:49–61. doi:10.1016/j.electacta.2012.04.044.
4. Flora SJS, Mittal M, Mehta A. Heavy metal induced oxidative stress & its possible reversal by chelation therapy. Indian J Med Res. 2008;128:501–23.
5. Li F, Wang J, Lai Y, Wu C, Sun S, He Y, Ma H. Ultrasensitive and selective detection of copper (II) and mercury (II) ions by dye-coded silver nanoparticle-based SERS probes. Biosens Bioelectron. 2013;39:82–7. doi:10.1016/j.bios.2012.06.050.
6. March G, Nguyen T, Piro B. Modified electrodes used for electrochemical detection of metal ions in environmental analysis. Biosensors. 2015;5:241–75. doi:10.3390/bios5020241.
7. Chauhan N, Pundir CS. An amperometric biosensor based on acetylcholinesterase immobilized onto iron oxide nanoparticles/multi-walled carbon nanotubes modified gold electrode for measurement of organophosphorus insecticides. Anal Chim Acta. 2011;701:66–74. doi:10.1016/j.aca.2011.06.014.
8. Ganjali MR, Motakef-Kazami N, Faridbod F, Khoee S, Norouzi P. Determination of Pb^{2+} ions by a modified carbon paste electrode based on multi-walled carbon nanotubes (MWCNTs) and nanosilica. J Hazard Mater. 2010;173:415–9. doi:10.1016/j.jhazmat.2009.08.101.
9. Adrrienne SE, Anne GW (2010) Guidelines for the identification and management of lead exposure in pregnant and lactating women.
10. Selvanayagam AS, Jeyaprakash BG, Rayappan JBB. Preparation, characterization and chemical sensing properties of polyaniline thin films. J Appl Sci. 2012;12:1710–3.
11. Liu C, Bai R, San Ly Q. Selective removal of copper and lead ions by diethylenetriamine-functionalized adsorbent: behaviors and mechanisms. Water Res. 2008;42:1511–22. doi:10.1016/j.watres.2007.10.031.
12. Gumpu MB, Sethuraman S, Krishnan UM, Rayappan JBB. A review on detection of heavy metal ions in water—an electrochemical approach. Sensors Actuators B Chem. 2015;213:515–33. doi:10.1016/j.snb.2015.02.122.
13. Prabhakaran D, Yuehong M, Nanjo H, Matsunaga H. Naked-eye cadmium sensor: using chromoionophore arrays of Langmuir-Blodgett molecular assemblies. Anal Chem. 2007;79:4056–65. doi:10.1021/ac0623540.
14. Narin I, Soylak M, Elçi L, Doğan M. Determination of trace metal ions by AAS in natural water samples after preconcentration of pyrocatechol violet complexes on an activated carbon column. Talanta. 2000;52:1041–6.
15. Pobozy E, Halko R, Krasowski M, Wierzbicki T, Trojanowicz M. Flow-injection sample preconcentration for ion-pair chromatography of trace metals in waters. Water Res. 2003;37:2019–26. doi:10.1016/S0043-1354(02)00615-2.

16. Gumpu MB, Nesakumar N, Sethuraman S, Krishnan UM, Rayappan JBB. Development of electrochemical biosensor with ceria–PANI core–shell nano-interface for the detection of histamine. Sensors Actuators B Chem. 2014;199:330–8. doi:10.1016/j.snb.2014.04.009.
17. Date Y, Terakado S, Sasaki K, Aota A, Matsumoto N, Shiku H, Ino K, Watanabe Y, Matsue T, Ohmura N. Microfluidic heavy metal immunoassay based on absorbance measurement. Biosens Bioelectron. 2012;33:106–12. doi:10.1016/j.bios.2011.12.030.
18. Nesakumar N, Sethuraman S, Krishnan UM, Rayappan JBB. Fabrication of lactate biosensor based on lactate dehydrogenase immobilized on cerium oxide nanoparticles. J Colloid Interface Sci. 2013;410:158–64. doi:10.1016/j.jcis.2013.08.009.
19. Zhuang J, Fu L, Tang D, Xu M, Chen G, Yang H. Target-induced structure-switching DNA hairpins for sensitive electrochemical monitoring of mercury (II). Biosens Bioelectron. 2013;39:315–9. doi:10.1016/j.bios.2012.07.015.
20. Wang Z, Qin Y, Wang C, Sun L, Lu X, Lu X. Preparation of electrochemical sensor for lead(II) based on molecularly imprinted film. Appl Surf Sci. 2012;258:2017–21. doi:10.1016/j.apsusc.2011.05.005.
21. Singh M, Nesakumar N, Sethuraman S, Maheswari U. Electrochemical biosensor with ceria—polyaniline core shell nano-interface for the detection of carbonic acid in blood. J Colloid Interface Sci. 2014;425:52–8. doi:10.1016/j.jcis.2014.03.041.
22. Simm AO, Banks CE, Wilkins SJ, Karousos NG, Davis J, Compton RG. A comparison of different types of gold-carbon composite electrode for detection of arsenic(III). Anal Bioanal Chem. 2005;381:979–85. doi:10.1007/s00216-004-2960-z.
23. Ilangovan R, Daniel D, Krastanov A, Zachariah C, Elizabeth R. Enzyme based biosensor for heavy metal ions determination. Biotechnol Biotechnol Equip. 2014;20:184–9. doi:10.1080/13102818.2006.10817330.
24. Shen L, Chen Z, Li Y, He S, Xie S, Xu X, Liang Z, Meng X, Li Q, Zhu Z, Li M, Le XC, Shao Y. Electrochemical DNAzyme sensor for lead based on amplification of DNA-au bio-bar codes. Anal Chem. 2008;80:6323–8. doi:10.1021/ac800601y.
25. Bagal-Kestwal D, Karve MS, Kakade B, Pillai VK. Invertase inhibition based electrochemical sensor for the detection of heavy metal ions in aqueous system: application of ultra-microelectrode to enhance sucrose biosensor's sensitivity. Biosens Bioelectron. 2008;24:657–64. doi:10.1016/j.bios.2008.06.027.
26. Chey CO, Ibupoto ZH, Khun K, Nur O, Willander M. Indirect determination of mercury ion by inhibition of a glucose biosensor based on ZnO nanorods. Sensors (Basel). 2012;12:15063–77. doi:10.3390/s121115063.
27. Soldatkin OO, Kucherenko IS, Pyeshkova VM, Kukla AL, Jaffrezic-Renault N, El'skayaa V, Dzyadevych SV, Soldatkin AP. Novel conductometric biosensor based on three-enzyme system for selective determination of heavy metal ions. Bioelectrochemistry. 2012;83:25–30. doi:10.1016/j.bioelechem.2011.08.001.
28. Upadhyay LSB. Urease inhibitors: a review. Indian J Biotechnol. 2012;11:381–8.
29. Guascito MR, Malitesta C, Mazzotta E, Turco A. Inhibitive determination of metal ions by an amperometric glucose oxidase biosensor. Sensors Actuators B Chem. 2008;131:394–402. doi:10.1016/j.snb.2007.11.049.
30. Solanki PR, Kaushik A, Agrawal VV, Malhotra BD. Nanostructured metal oxide-based biosensors. NPG Asia Mater. 2011;3:17–24. doi:10.1038/asiamat.2010.137.
31. Benini S, Rypniewski WR, Wilson KS, Miletti S, Ciurli S, Mangani S. A new proposal for urease mechanism based on the crystal structures of the native and inhibited enzyme from Bacillus pasteurii: why urea hydrolysis costs two nickels. Structure. 1999;7:205–16. doi:10.1016/S0969-2126(99)80026-4.
32. Ciurli S, Benini S, Rypniewski WR, Wilson KS, Miletti S, Mangani S. Structural properties of the nickel ions in urease: novel insights into the catalytic and inhibition mechanisms. Coord Chem Rev. 1999;190–192:331–55. doi:10.1016/S0010-8545(99)00093-4.
33. Begum A, Ramaiah M, Harikrishna KI, Veena K. Heavy metal pollution and chemical profile of Cauvery River water. E-Journal Chem. 2009;6:47–52. doi:10.1155/2009/154610.
34. Jameel AA, Sirajudeen J, Abdul R. Studies on heavy metal pollution of ground water sources between Tamilnadu and Pondicherry, India. Adv Appl Sci Res. 2012;3:424–9.
35. Bui MPN, Li CA, Han KN, Pham XH, Seong GH. Electrochemical determination of cadmium and lead on pristine single-walled carbon nanotube electrodes. Anal Sci. 2012;28:699–704.
36. Li Y, Liu XR, Ning XH, Huang CC, Zheng JB, Zhang JC. An ionic liquid supported CeO_2 nanoparticles–carbon nanotubes composite-enhanced electrochemical DNA-based sensor for the detection of Pb^{2+}. J Pharm Anal. 2011;1:258–63. doi:10.1016/j.jpha.2011.09.001.
37. Hwang GH, Han WK, Park JS, Kang S-G. An electrochemical sensor based on the reduction of screen-printed bismuth oxide for the determination of trace lead and cadmium. Sensors Actuators B Chem. 2008;135:309–16. doi:10.1016/j.snb.2008.08.039.
38. Wang Z, Wang H, Zhang Z, Liu G. Electrochemical determination of lead and cadmium in rice by a disposable bismuth/electrochemically reduced graphene/ionic liquid composite modified screen-printed electrode. Sensors Actuators B Chem. 2014;199:7–14. doi:10.1016/j.snb.2014.03.092.
39. Yusof NA, Daud N, Zareena S, Saat M, Tee TW. Electrochemical characterization of carbon nanotubes / nafion / aspartic acid modified screen printed electrode in development of sensor for determination of Pb(II). Int J Electrochem Sci. 2012;7:10358–64.
40. Huang MR, Ding YB, Li XG. Combinatorial screening of potentiometric Pb(II) sensors from polysulfoaminoanthraquinone solid ionophore. ACS Comb Sci. 2014;16:128–38. doi:10.1021/co400140g.
41. Domínguez-Renedo O, Alonso-Lomillo MA, Ferreira-Gonçalves L, Arcos-Martínez MJ. Development of urease based amperometric biosensors for the inhibitive determination of Hg (II). Talanta. 2009;79:1306–10. doi:10.1016/j.talanta.2009.05.043.